- 11 -
MICROPHONES

ACOUSTIC RECEIVERS

Up to this point we have talked almost exclusively about transducers for generating sound. It may well be the case that there are more microphones used per annum than loudspeakers and as such the topic warrants our discussion. Thankfully the two devices bear a high degree of similarity and our T-matrix approach will be work just as effectively on microphones as it did on loudspeakers. The fact is that with the tools that we have already developed there is only a small difference in the approach and calculations required to analyze a microphone. Given this situation we can round out our study with little addition complexity.

11.1   Background

Many years ago there were many different kinds of microphone, each with a different motor structure, diaphragm configuration, etc. In the recent past, however, the invention of the Electret microphone has made all other designs obsolete. While some designs of the moving coil variety still survive they are not of sufficient usage to warrant detailed study here. By developing the theory for the Electret microphone, by far the most common, it is a simple matter to replace the Electret "motor" by a moving coil if that is so desired.
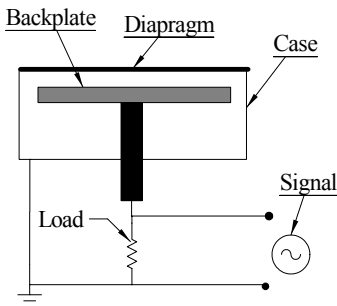

Figure 11-1 - Schematic drawing of a microphone

The Electret is basically a self energized motor, much like that of a permanent magnet, except that the potential is electric not magnetic. We have already seen the derivation of the electrostatic motor structure in Sec.2.4 on page 34. In this section we will use those results to show their application to a microphone. Fig.11-1 shows the basic layout of an Electret microphone structure. The backplate is covered in Teflon, which is then "charged" with a high potential electron gun – basically electrons are imbedded into the Teflon. This leaves a high charge potential on the Teflon resulting in the static polarizing voltage E.

The diaphragm is usually grounded and the backplate is coupled to ground through a resistance, usually very large for reasons that we shall soon see. As the diaphragm moves the capacitance changes and since the voltage is constant, the charge on the plates must vary. The T-matrix for this motor is shown below.

$$\begin{pmatrix} F(\omega) \\ V(\omega) \end{pmatrix} = \begin{pmatrix} 1 & z_m + \dfrac{1}{i\omega C_{me}} \\ 0 & 1 \end{pmatrix} \begin{pmatrix} C_0 \dfrac{E_0}{d} & 0 \\ 0 & \dfrac{d}{C_0 E_0} \end{pmatrix} \begin{pmatrix} 1 & 0 \\ -i\omega C_0 & 1 \end{pmatrix} \begin{pmatrix} E(\omega) \\ I(\omega) \end{pmatrix} \qquad (11.1.1)$$

At this point, it should be obvious that all we need is a simple mechanical-acousti-cal coupling matrix to precede the above equation and we have a simple micro-phone with sound pressure as the input and a voltage as the output. The voltage outputs that result are exceedingly small and so virtually all Electret microphones have an on-board voltage follower to increase the available current and decrease the source impedance.

One of the principal design considerations for microphones is the noise level, and its spectrum. The follower circuit can have a significant effect on this noise floor, but it can also be designed in such a way as to be a negligible source of noise. We will first consider where the primary source of noise is in a microphone.

11.2   Microphone Noise

The main source of microphone noise is the thermal noise of its internal mechanics. Consider the fundamental equation for thermal noise[1]

$$E_t = \sqrt{4kTR\Delta f} \qquad (11.2.2)$$

E_t = *rms thermal noise voltage* (Volts /$\sqrt{\text{Hz}}$)

T = *temperature in Kelvin's* (°K)

K = *Boltzmans constant = 1.38 x 10-23* W-s/°K

R = *the resistance (or more appropriately the real part of the circuit)*

Δf = *the bandwidth* (Hz)

From the standpoint of the output electrical signal, the noise depends on the cir-cuit shown in Fig. 11-1 as seen looking in from the electrical output – the parallel combination of the diaphragm capacitance and the load resistance. The real part of this combination is

$$\mathbb{R}\left(\frac{1}{R} - i\omega C_0\right)^{-1} = \frac{R}{1 + \omega^2 C_0^2 R^2} \qquad (11.2.3)$$

From this result we can see an interesting fact. Fig. 11-2 shows this function for $R = C_0 = 1$. Above $\omega = C_0 R$, in this normalized curve, the noise looks like $1/f$

---

1. See Motchenbacher, *Low Noise Electronic System Design*
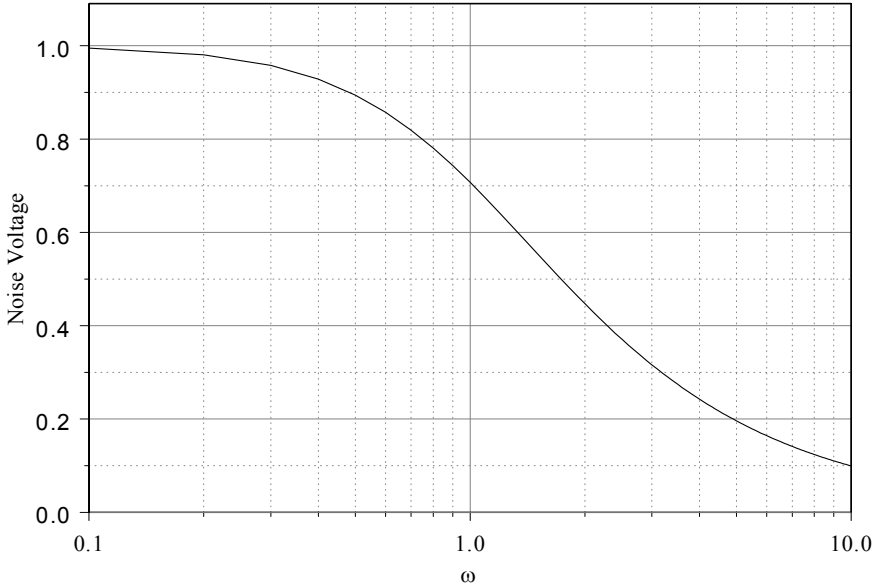
Figure 11-2 - Noise voltage versus frequency

noise which is proportional to $1/\sqrt{R}\,C_0$. As the microphone gets smaller, C_0 must decrease and the noise will increase in level and become predominately $1/f$. This means that small microphones <u>must</u> get noisier since as the diaphragm area decreases – the noise figure is going up and, of course, the signal level is going down. This occurs regardless of any electronic noise in the preamp, etc. This noise level is thermal noise in the sensor itself and cannot be alleviated with any physically available technique (except lowering the temperature, which in a small unit is not very practical.) This fundamental relationship between the microphone noise and its size has often been overlooked.

Of course, it is also obvious that increasing R has the opposite effect and in any microphone the largest R practical is usually used. It is not uncommon to see R values in the Tera-ohms. At these levels, leakage resistance becomes a critical factor. It should also be apparent that the diaphragm capacitance should be composed of predominately signal generating capacitance – parasitic capacitance decreases the signal without decreasing the noise. Since typical diaphragm capacitance values for a ¼" microphone might be

$$C_0 = \frac{\varepsilon_0 \pi r^2}{d} \simeq 50\,\text{pF}$$

(11.2.4)

any stray capacitance must be tightly controlled if low noise is an objective.

There is also noise from the acoustical circuit to worry about. This effect is easily added to our analysis. The noise figure shown in Eq.(11.2.2) can be applied to the entire input circuit, including the acoustical network. So we simply compile

the entire T-matrix, extract the impedance seen looking into the device and takes the real part.

Lastly, there is the noise of the preamp to consider. The preamp is usually located as close to the backplate as possible since any capacitance or resistance to the input of the preamp tends to degrade the SNR. With a modern low noise FET located inside the microphone capsule the preamp noise can be made to be a negligible portion of the total noise, which will be dominated by the sensor noise.

11.3   A Microphone Example

As an example of the techniques described here, consider the device shown in Fig. 11-3. We want to calculate $E_{out}(f)$ (for a flat pressure at the input port) and the noise spectrum. We have selected this device because it will be a good example for the use of the techniques that we have developed and it is a device not unlike many that are used quite often in practice.

Figure 11-3 -   Microphone example

For this example, we will suppose that

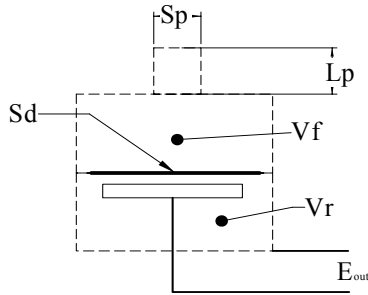|		
S_p = .5 mm²	V_f = 40 mm³	E_0 = 350 volt
L_p = 1 mm	V_r = 20 mm³	f_0 = 5kHz (*resonance*
S_d = 10 mm²	d = .01 mm	*with rear volume*)

Linking together the T-matrices leads to

$$\begin{pmatrix} P(\omega) \\ U(\omega) \end{pmatrix} = [Port][Vf][Sd][mech.+Vr][electrical]\begin{pmatrix} E(\omega) \\ I(\omega) \end{pmatrix} \tag{11.3.5}$$

which, when multiplied out yields an algebraic result, is, unfortunately, too long to write out.

When normalized, the numerator of the pressure to voltage transfer function is equal to

$$\varepsilon_0^2 \left(\frac{S_d}{d} \right)^3 E_0 \tag{11.3.6}$$

This equation shows how strongly dependent the output is on diaphragm area. It is just as highly dependent on the gap. The gap, d, cannot remain at the same value as S_d is increased because of the strong electrostatic pull of the static electric field, which causes the diaphragm to sag towards the backplate. The sag becomes greater with larger area and as such d must be increased as S_d increases, fortu-

nately, not at the same rate or we would never get anywhere. Of course, the ability to control small gaps is an industry goal. One of the most serious problems in practice is that the diaphragm materials can be highly sensitive to temperature and humidity, making for a device which can easily become uncalibrated or the diaphragm can even collapse onto the backplate, completely shorting out the output.

The output is also proportional to the polarizing voltage, E_0. For Electrets this is a fairly fixed quantity, but with external power supplies this number can go very high. There is little power supply rejection so the supply must be very clean.

Fig. 11-4 shows the response for this unit, with the variables set as defined above. The first thing to notice is that it is not difficult to get an almost ideal response curve (except for the high end, which, as we will see, is easily controllable). The load resistance causes a low frequency fall off – a HP filter and demonstrates the need for very large resistance values to load the device.

It should also be obvious that with load resistances as high as $100G\Omega$ the preamplifier following the sensor must have a very large input impedance, hopefully much larger than $100G\Omega$ – a difficult task. An FET is usually mounted directly on the backplate to avoid parasitic elements that reduce the signal but not the noise.

Our example is deliberately sub-optimal in order to show some features of these devices. First, we can see that the acoustic resonance has a high Q owing to the fact there is little electromagnetic damping. For this reason, the port usually
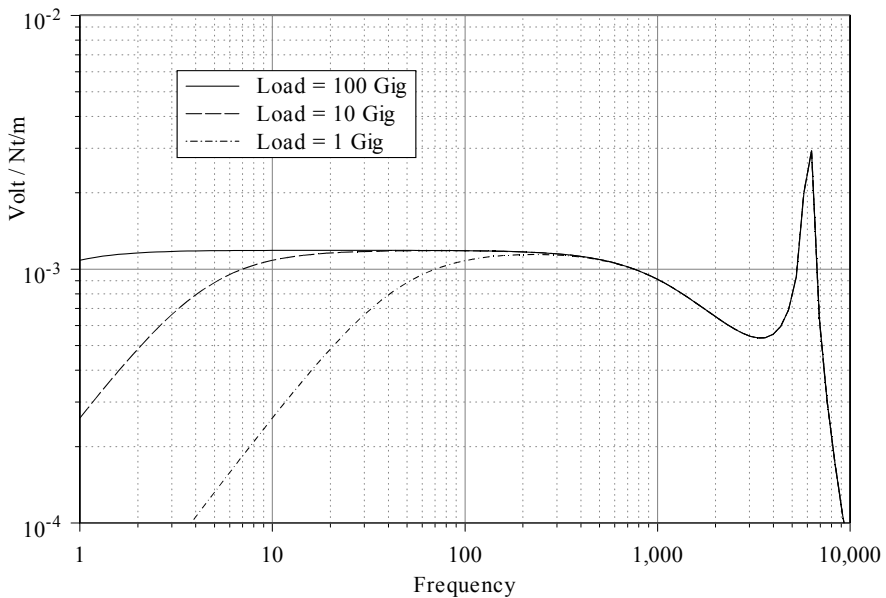

Figure 11-4 - A typical small microphone example

has a damper placed in it. Above the acoustic resonance, the output drops very fast and the device ceases to be usable.

The output falls slightly above the diaphragm resonance, which is lowered by the electrostatic coupling (it is mechanically at about 5 kHz). The diaphragm resonance is usually fairly well damped owing to the very small gap which yields a great deal of mechanical damping. Holes in the backplate can increase this damping, but at the loss of output – a trade-off, if required. Placing the mechanical resonance, as well as the acoustic one, out-of-band (unlike the example shown here) is a relatively easy thing to do, making the response of this device almost perfect.

The noise spectrum can be calculated by looking back into the same set of T-matrices that we used above and dividing the voltage terms by the current terms and taking the real part. This value is then used in Eq. (11.2.2) to plot the noise power spectrum.
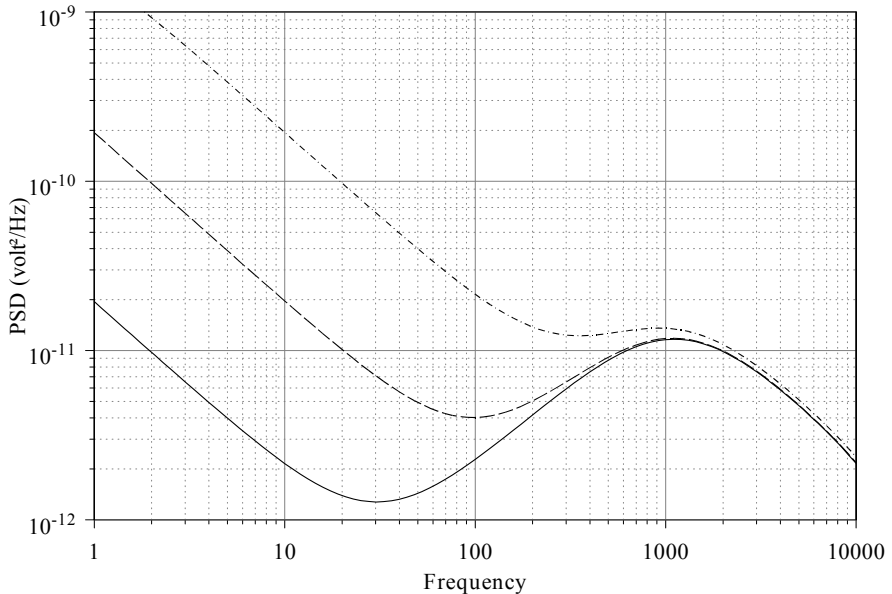

Figure 11-5 - Noise power spectrum

Fig. 11-5 shows the noise Power Spectral Density (PSD) function for the same load resistance values as in the previous figure. The effect of the load resistance can clearly be seen at the lower end of this curve. The noise increases with lower resistance values while the output decreases, resulting in a substantial reduction in Signal to Noise Ratio (SNR). The importance of a very high load resistance is clear. One must be careful when looking at a spectrum like that shown above, because it can be misleading. The RMS noise value is the square root of the area under the PSD curve, *plotted in linear coordinates*. This makes the differences in the

three curves substantially smaller than they appear in log coordinates. The RMS noise is dominated by the hump in the noise curve at 1 kHz.

This hump is the result of the thermal noise of the diaphragm's mechanical impedance. This is why it is not greatly affected by the electrical load. This noise, which dominates the RMS noise level, will increase as the diaphragm area goes down, making the usable SNR of the device almost completely dominated by the physical size of the microphone. This is a situation for which there is no solution.

11.4 Microphone Enclosures

The microphone's enclosure is the only feature that has any real effect on its response. There are, of course, an infinite number of different shapes and sizes that one could use here. Interestingly enough, one of the more important enclosure shapes turns out to be one that we have already developed the machinery to handle – a sphere. We could make the sphere small, just large enough to contain the element, but that would end up having little effect and would not be too interesting. On the other hand, we could make the sphere the size of a human head and place the microphone at the ear position and get an interesting result. We will do the latter.

The problem now at hand is somewhat different than the one that we had done in Sec. 3.4. We are now interested in the scattering of a plane wave of sound incident on a sphere from which we will find the pressure at a point on the surface of the sphere (or we could do an average if required) and use this as the input to our model.

In order to proceed, we will need to match the wave functions for a plane wave to the spherical boundary conditions. The expansion of a plane wave into spherical modes is well know[2]

$$p_{plane} = P_0 e^{ikr\cos\theta} = P_0 \sum_{m=0}^{\infty} (2m+1)i^m P_m(\cos\theta) j_m(kr) \qquad (11.4.7)$$

where these functions are all known to us. Fitting this to a rigid sphere of radius a

$$v_a = -i\rho c \frac{\delta p_a}{\delta r} = -i\rho c \frac{\delta}{\delta r}\left(p_{plane} + p_s\right) = 0 \bigg|_{r=a} \qquad (11.4.8)$$

p_a = *the pressure on the surface of the sphere*

p_s = *the pressure of the scattered wave*

v_a = *the radial velocity at the surface of the sphere*

Applying the boundary conditions we have

---

2. See Morse, (any text)

$$\frac{\delta p_s}{\delta r} = -\frac{\delta p_{plane}}{\delta r}$$

$$\frac{1}{k}\sum_{m=0}^{\infty} A_m P_m(\cos\theta)h_m^{'}(ka) = P_0 \frac{1}{k}\sum_{m=0}^{\infty}(2m+1)i^m P_m(\cos\theta)j_m^{'}(ka) \qquad (11.4.9)$$

from which orthogonality tells us

$$p_s = \sum_{m=0}^{\infty}(2m+1)i^m P_m(\cos\theta)\frac{j_m^{'}(ka)}{h_m^{'}(ka)}h_m(kr) \qquad (11.4.10)$$

and the pressure at the surface of the sphere then becomes

$$p_a(\theta) = \sum_{m=0}^{\infty}(2m+1)i^m P_m(\cos\theta)\left(\frac{j_m^{'}(ka)}{h_m^{'}(ka)}h_m(ka) + j_m(ka)\right) \qquad (11.4.11)$$

Fig. 11-6 shows the polar map for the pressure on the surface of a sphere in the sound field of a distant source at 0°. Each level is -6 dB. For a sphere the size of a head, the upper frequency limit ($ka = 26$) is about 10 kHz. The astute observer will recognize this map as an approximation to the Head Related Transfer Function (HRTF), excluding the pinna and ear canal.
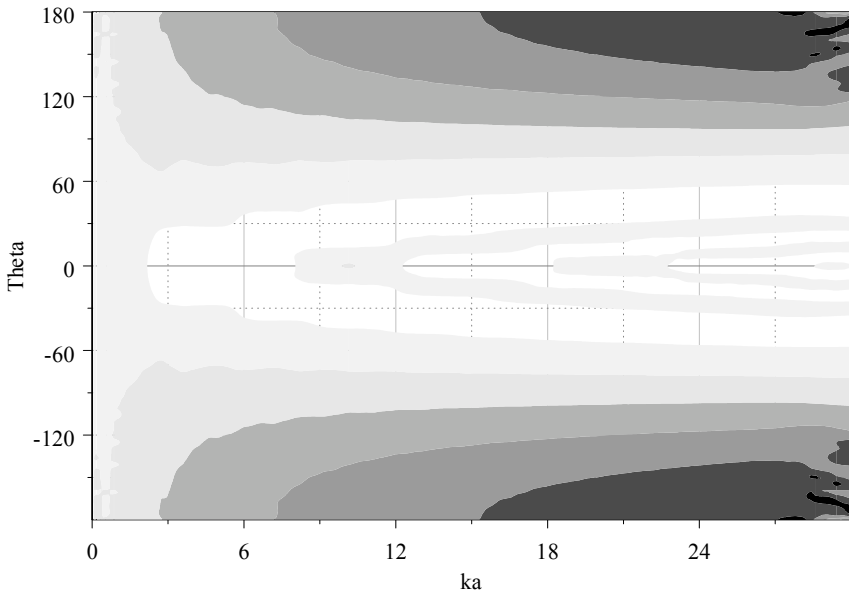

Figure 11-6 - Polar map for pressure on the surface of a sphere

For a small cartridge microphone, 10 kHz would occur at

$$ka = \frac{2\pi(10,000\,\text{Hz.})}{343\text{ m/s}}.02\,\text{m} = 3.7$$

Since a microphone has almost no frequency response of its own, the frequency response will be dominated by that of the spherical diffraction shown in Fig. 11-6. For a 4 cm diameter sphere, (a typical microphone capsule) there will be almost no effect at all on the axial response. A slight rise in the response will occur at the high end, but there will be a substantial narrowing of the polar pattern.

11.5   Microphone Pattern Control

The subject of microphone polar pattern control is extensive and since microphones are not the central subject of this text, we will only briefly review the subject. We will show a general approach that can be used to synthesize nearly any polar pattern.

Patterns in microphones are, like nearly everything else that we have studied, a modal problem. A microphone can be of two varieties: a monopole or a dipole. Think of these as the $P_0(\cos\theta)$ and $P_1(\cos\theta)$ modes. We can construct a variety of polar patterns from just these two elements.

Fig. 11-7 shows a small set of the possible polar patterns available by summing a monopole and a dipole with varying amplitudes. The dipole in this figure is added with amplitudes .4, .6, .8, 1.0 and 1.2. The 1.0 curve is called cardiod and the 1.2 curve is close to a hyper-cardiod pattern. It is also possible to achieve a cardiod pattern by a judicious sum of front and rear diaphragm pressures.
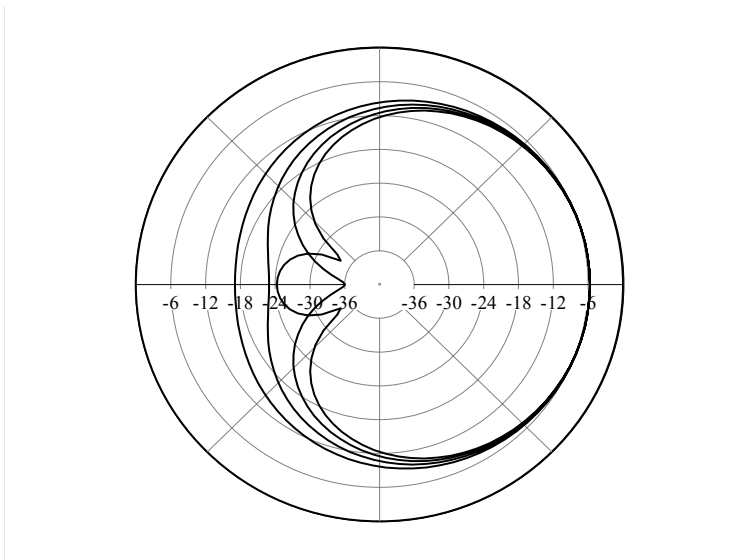

Figure 11-7 - Polar patterns for first two modes.

Consider a complex sum of front and rear sound pressure

$$p_{total} = p_{front} - a \cdot p_{rear}$$

(11.5.12)

$a = some \; complex \; amplitude$

We know that the polar pattern of a cardiod is

$$P_0(\cos\theta) + P_1(\cos\theta) = 1 + \cos\theta$$

(11.5.13)

and a little thought (well maybe more than a little) will show that this can also be written as

$$\frac{1 + e^{i\pi/2 \cos\theta + i\pi/2}}{2}$$

(11.5.14)

If we can arrange to have two delays, one that is a constant $\pi/2$ and the other that varies with angle then we can build a cardiod with a single diaphragm. This can be achieved as shown in Fig.11-8, where a long tube has its opening located a distance
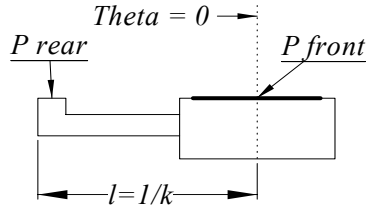

Figure 11-8 - Cardiod microphone port arrangement

$$l = \frac{1}{k} = \frac{3c}{2\pi f_{max}}$$

(11.5.15)

f_{max} = the maximum frequency of desired control.

There will be a constant delay down the tube and a delay based on θ due to the spacing. The results for the polar map are shown in Fig.11-9, where we can see that the cardiod pattern holds over a fairly wide frequency range so long as $kl < 3$. The polar pattern gets wider at the high end of the control range and breaks down completely at $kl = 3$, where there are two main lobes of more than 6 dB greater than the axial response. Above $kl = 3$, multiple lobes begin forming.

We will finish up this chapter with a brief discussion of how we might create any desired pattern with a multiplicity of microphone elements. With the low cost of Electret devices these large element arrays are quite practical.

11.6 Microphone Arrays

It would seem logical to introduce this section with a discussion of a microphone line array. We could describe how the directional response is the Fourier Transform of the array shading (the amplitude of the individual elements) but in light of the work that we have already done for radiating arrays', this is almost a trivial exercise. It should also be obvious that the polar pattern of a two dimensional array of elements is the two dimensional transform of the element weighting. Nothing new here either. The only thing that one might encounter in the
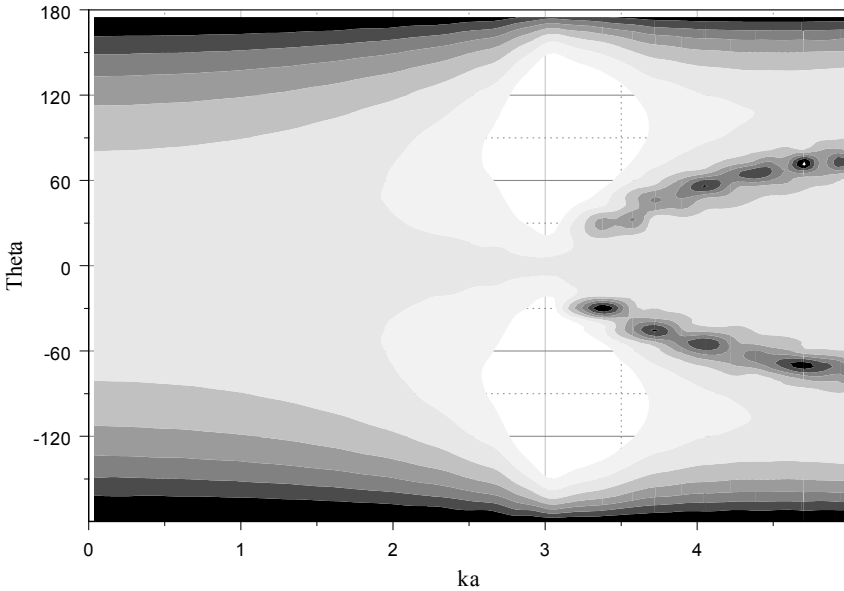
Figure 11-9 - Polar map for cardiod microphone

microphone case is the fact that it is possible to hypothesize polar reception patterns that would translate into complex coefficients after taking the Fourier Transform. This is really no problem if we simply interpret the complex part as a time delay. In this way, we could synthesize end-fired arrays, shotgun microphones, etc. There are many examples of this application.

A more interesting example for us occurs if we look at the spherical case. Consider a sphere of radius a. It needn't really be a sphere. The important factor is the fact that the microphones are spaced apart by a distance $2a$. If we select a polar pattern from the range of patterns available as Legendre Polynomials (see Fig. 3-3 on page 52), then the design task becomes relatively easy. Take the case of $P_2(\cos\theta)$, which has four lobes. The two side lobes are out of phase from the other two. The lobes also have different amplitudes. If we take as the element weighting the values of the lobes and place microphones at the angular location of the lobes peak values, then we will get the directivity pattern of $P_2(\cos\theta)$, or at least as close as we can get with a finite number and size of elements. It is more interesting, however, to modify our problem slightly.

It would be more desirable to only have a major directivity lobe in the frontal direction, no lobe in the rear. We can modify the pattern by simply adding a dipole term which will reduce the rear lob to zero (much like the cardiod case). In mathematical form, what we are saying is

$$P_2(\cos\theta) + P_1(\cos\theta) = \left(\tfrac{3}{4}\cos 2\theta + \cos\theta + \tfrac{1}{4}\right) \tag{11.6.16}$$

which is zero when $\theta = \pi$. If we normalize this form to have a value of one when $\theta = 0$, then we get

$$\left(\tfrac{3}{8}\cos 2\theta + \tfrac{1}{2}\cos\theta + \tfrac{1}{8}\right) \tag{11.6.17}$$

evaluating this equation at the locations of the elements $\theta = 0,\ \pi/2,\ \pi, -\pi/2$ we will get the value for the weights of the elements.

$mic\ 1 = 1.0$

$mic\ 2 = mic\ 4 = -.125$

$mic = 0.0$

We find that we really only need three microphones to get an even better directivity than we had hoped for with four. The polar response map is shown in Fig. 11-10. The directivity control acts over a wide range but the response falls off at the
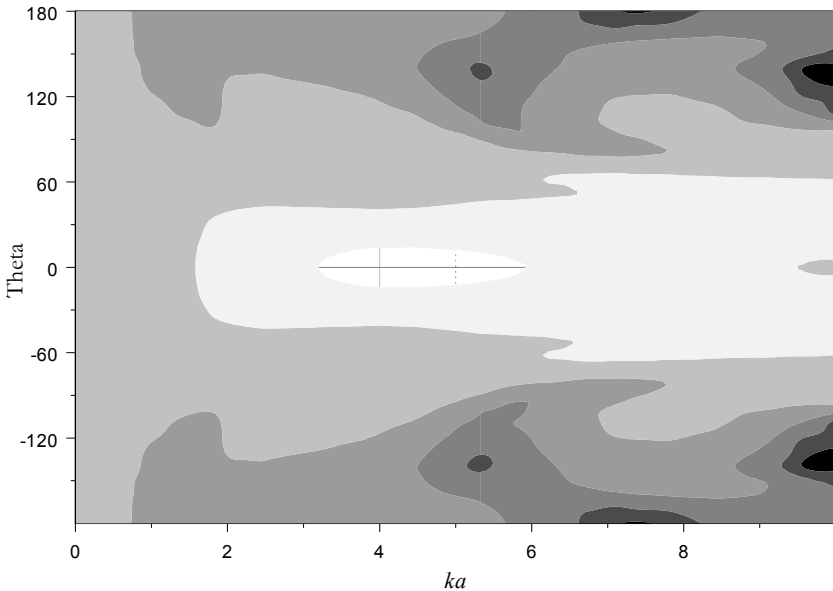

Figure 11-10 - Polar map for spherical microphone array

higher and lower frequencies. We have not normalized the axial response to flat in this plot.

Generally, one would not need to place the microphones in a circle as in this example. If directivity were desired in only one direction then we would prefer a simple line array. But the circle offers a unique opportunity if the desired direction of maximum reception is changing, like in a conference room where one might want to steer the array to the current speaker. With electronic control (or mechanical but with more limited control), these four elements could be readily steered in

any direction by a continuous amplitude summing of the microphone signals. This could even be automated to follow the talker no matter where they were – an adaptive signal processing application beyond the scope of our text here.

11.7   Summary

We have shown that microphones bear a strong similarity to sound radiating transducers and that the physics of the problems are almost identical. The same tools that served us so well in the radiation problems for sound emitting devices have also given us a good start on the reception ones as well.